

Supporting Materials (SM)

Temperature-induced morphological transformation of SDS micelles: The fracto-eutectogel to fluid transition

Lauren Matthews^{1,2,†}, Sarah E.S. Michel¹, Sarah E. Rogers³, Paul Bartlett¹, Andrew J. Johnson⁴, Robert Sochon⁴, and Wuge H. Briscoe^{1}*

¹ School of Chemistry, University of Bristol, Cantock's Close, Bristol, BS8 1TS, UK.

² Bristol Centre for Functional Nanomaterials, HH Wills Physics Laboratory, University of Bristol, Tyndall Avenue, Bristol, BS8 1TL, UK.

³ ISIS Muon and Neutron Source, Rutherford Appleton Laboratory, Harwell Oxford, Didcot, OX11 0QX, UK.

⁴ GlaxoSmithKline, St George's Avenue, Weybridge, KT13 0DE, UK.

*Corresponding author; email: wuge.briscoe@bristol.ac.uk; Tel: +44 (0) 117 331 8256

[†] Current address: ESRF, The European Synchrotron, 38043 Grenoble, France.

S1. Probing the temperature-induced gel to fluid transition with PLM

Figure S1 shows the PLM images of the phase transition at finer temperature increments, $T = 50 - 55\text{ }^{\circ}\text{C}$, capturing the disappearance of the fractal aggregates. **Figure S2** shows the effect of temperature on the fracto-eutectogel as the temperature is increased in $5\text{ }^{\circ}\text{C}$ increments.

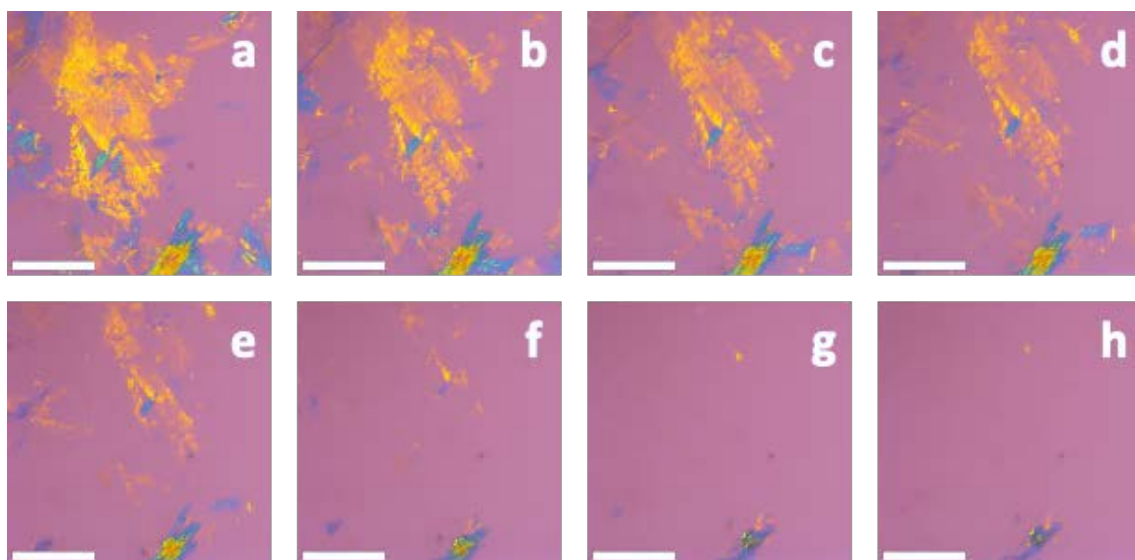


Figure S1 PLM images of 2.5 wt% SDS in glyceline between $T = 50 - 55\text{ }^{\circ}\text{C}$ at a small temperature increment step ($< 1\text{ }^{\circ}\text{C}$ per image), showing the disappearance of the fractal aggregates. Images are taken at 4 x magnification with a 530 nm first order waveplate, temperatures are indicated, and scale bars represent $100\text{ }\mu\text{m}$.

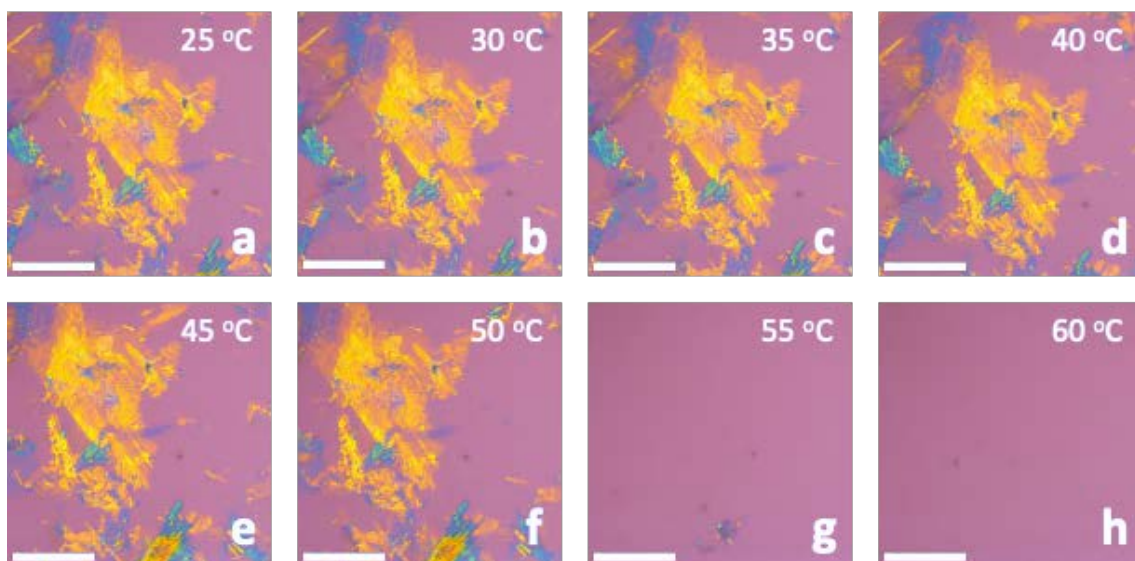


Figure S2 PLM images of 2.5 wt% SDS in glyceline at different temperatures, showing the disappearance of the fractal aggregates with elevated temperature. Images are taken at 4 x

magnification with a 530 nm first order waveplate, temperatures are indicated, and scale bars represent 100 μm .

S2. Model refinement for SANS data fitting of the SDS-in-glyceline gel at 70 °C

The higher T SANS profiles of the SDS-in-glyceline gel indicated the formation of globular aggregates, so four globular micelle models on SasView were trialed to find the most appropriate model for the system (**Figure S3**), with tables summarising the fitting parameters for each (**Table S1** - **Table S4**). Of the four globular micelle models trialed, the spherical and cylindrical models were shown to have the best fits with sensible physical parameters.

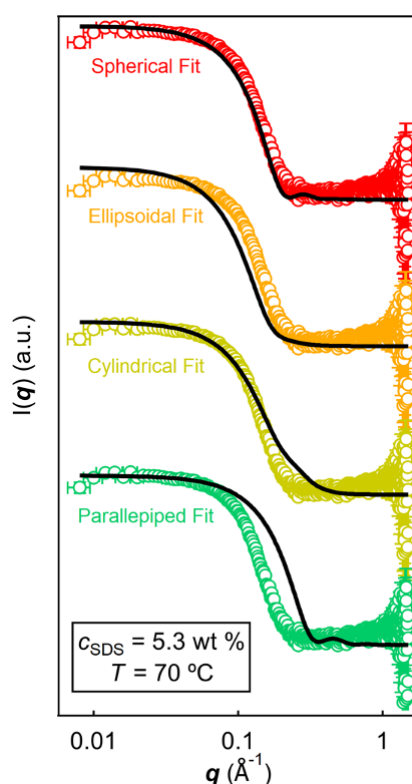


Figure S3 Fitted SANS data for 5.3 wt % SDS in glyceline at 70 °C using: a spherical model (red), an ellipsoidal model (orange), a cylindrical model (yellow), and a parallelepiped fit (green).

Table S1 Fitting parameters for the sphere model used to simulate the data for 5.3 wt % h -SDS in d -glyceline at 70 °C: radius r , scattering length density of SDS ρ_{SDS} , scattering length density of glyceline ρ_{Gly} , polydispersity of the radius σ_r , and chi squared value χ^2 .

Sphere Model	5.3 wt %
r (Å)	19.8
ρ_{SDS} (10^{-6} Å ⁻²)	0.50

$\rho_{\text{Gly}} (10^{-6} \text{ \AA}^{-2})$	5.80
σ_r	0.08
χ^2	10.8

Table S2 Fitting parameters for the ellipsoid model used to simulate the data for 5.3 wt % *h*-SDS in *d*-glyceline at 70 °C: polar radius r_P , equatorial radius r_E , scattering length density of SDS ρ_{SDS} , scattering length density of glyceline ρ_{Gly} , polydispersity of the polar radius σ_P , polydispersity of the equatorial radius σ_E , and chi squared value χ^2 .

Ellipsoid Model	5.3 wt %
$r_P (\text{\AA})$	21.5
$r_E (\text{\AA})$	19.5
$\rho_{\text{SDS}} (10^{-6} \text{ \AA}^{-2})$	0.493
$\rho_{\text{Gly}} (10^{-6} \text{ \AA}^{-2})$	5.601
σ_P	0.31
σ_E	0.31
χ^2	2.45

Table S3 Fitting parameters for the cylinder model used to simulate the data for 5.3 wt % *h*-SDS in *d*-glyceline at 70 °C: cylinder radius r , length l , scattering length density of SDS ρ_{SDS} , scattering length density of glyceline ρ_{Gly} , polydispersity of the radius σ_r , polydispersity of the length σ_l , and chi squared value χ^2 .

Cylinder Model	5.3 wt %
$r (\text{\AA})$	20.0
$l (\text{\AA})$	14.0
$\rho_{\text{SDS}} (10^{-6} \text{ \AA}^{-2})$	0.395
$\rho_{\text{Gly}} (10^{-6} \text{ \AA}^{-2})$	5.788
σ_r	0.0
σ_l	0.0
χ^2	11.6

Table S4 Fitting parameters for the parallepiped model used to simulate the data for 5.3 wt % *h*-SDS in *d*-glyceline at 70 °C: length of side a l_a , length of side b l_b , length of side c l_c , scattering length density of SDS ρ_{SDS} , scattering length density of glyceline ρ_{Gly} , polydispersity of side a σ_a , polydispersity of the side b σ_b , polydispersity of the side c σ_c and chi squared value χ^2 .

Parallepiped Model	5.3 wt %
l_a (Å)	20.0
l_b (Å)	20.0
l_c (Å)	20.0
ρ_{SDS} (10^{-6} Å ⁻²)	0.395
ρ_{Gly} (10^{-6} Å ⁻²)	5.788
σ_a	0.1
σ_b	0.1
σ_c	0.1
χ^2	118.2

The spherical and cylindrical models were then further refined to find the most appropriate model (**Figure S4**), with the fit parameters (**Table S5 - Table S6**). The core-shell-cylinder model showed the most appropriate fit, determined by a combination of the χ^2 value and the physical parameters. Therefore, the core-shell-cylinder model was chosen as the structure for the higher T SANS profiles.

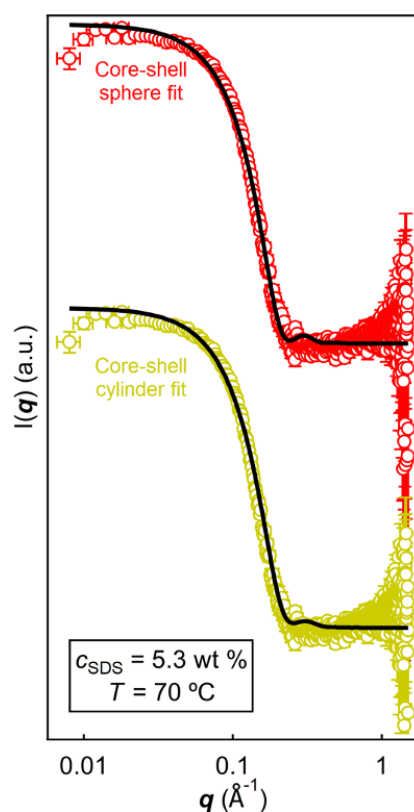


Figure S4 Refined fitted SANS data for 5.3 wt % SDS in glyceline at 70 °C using: a spherical model (red), and a cylindrical model (yellow).

Table S5 Fitting parameters for the core-shell-sphere model used to simulate the data for 5.3 wt % *h*-SDS in *d*-glyceline at 70 °C: radius r , thickness t , scattering length density of the core ρ_{core} , scattering length density of the shell ρ_{shell} , scattering length density of glyceline ρ_{Gly} , polydispersity of the radius σ_r , polydispersity of the thickness σ_t , and chi squared value χ^2 .

Core-Shell-Sphere Model	5.3 wt %
r (Å)	18.2
t (Å)	3.6
ρ_{core} (10^{-6} Å^{-2})	-0.391
ρ_{shell} (10^{-6} Å^{-2})	5.024
ρ_{Gly} (10^{-6} Å^{-2})	5.842
σ_r	0.077
σ_t	~ 0.0
χ^2	2.45

Table S6 Fitting parameters for the core-shell-cylinder model used to simulate the data for 5.3 wt % *h*-SDS in *d*-glyceline at 70 °C: core radius r , shell thickness t , cylinder length l , scattering length density of the core ρ_{core} , scattering length density of the shell ρ_{shell} , scattering length density of glyceline ρ_{Gly} , polydispersity of the core radius σ_r , polydispersity of the shell thickness σ_t , polydispersity of the cylinder length σ_l , and chi squared value χ^2 .

Core-Shell-Cylinder Model	5.3 wt %
r (Å)	16.3
t (Å)	4.8
l (Å)	23.9
ρ_{core} (10^{-6} Å^{-2})	-0.38
ρ_{shell} (10^{-6} Å^{-2})	4.80
ρ_{Gly} (10^{-6} Å^{-2})	5.87
σ_r	0.05
σ_t	0.05
σ_l	0.05
χ^2	2.45

S2. The cylinder to sphere transition at 0.6 wt % SDS in glyceline

The transition from a core-shell-cylinder structure to a core-shell-sphere structure was observed at $c_{\text{SDS}} = 0.6$ wt %, this was trialled with both models first before deciding on a morphology (**Figure S5**), with the fit parameters (**Table S7 - Table S8**). From this fitting analysis, the most appropriate structure was found to be a core-shell-sphere model and thus, this was the chosen structure for this c_{SDS} at elevated T .

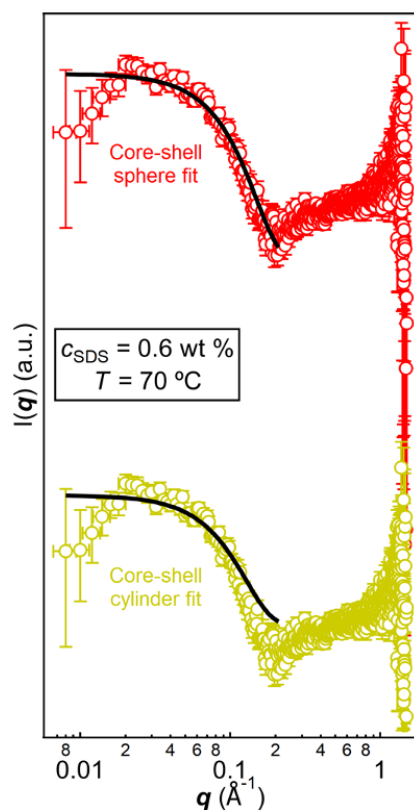


Figure S5 Refined fitted SANS data for 0.6 wt % SDS in glyceline at 70 °C using: a spherical model (**red**), and a cylindrical model (**yellow**).

Table S7 Fitting parameters for the core-shell-sphere model used to simulate the data for 0.6 wt % *h*-SDS in *d*-glyceline at 70 °C: radius r , thickness t , scattering length density of the core ρ_{core} , scattering length density of the shell ρ_{shell} , scattering length density of glyceline ρ_{Gly} , polydispersity of the radius σ_r , polydispersity of the thickness σ_t , and chi squared value χ^2 .

Core-Shell-Sphere Model	0.6 wt %
r (Å)	16.4
t (Å)	5.0
ρ_{core} (10^{-6} Å^{-2})	-0.300
ρ_{shell} (10^{-6} Å^{-2})	5.185
ρ_{Gly} (10^{-6} Å^{-2})	5.742
σ_r	0.05
σ_t	0.05
χ^2	1.35

Table S8 Fitting parameters for the core-shell-cylinder model used to simulate the data for 0.6 wt % *h*-SDS in *d*-glyceline at 70 °C: core radius r , shell thickness t , cylinder length l , scattering length density of the core ρ_{core} , scattering length density of the shell ρ_{shell} , scattering length density of glyceline ρ_{Gly} , polydispersity of the core radius σ_r , polydispersity of the shell thickness σ_t , polydispersity of the cylinder length σ_l , and chi squared value χ^2 .

Core-Shell-Cylinder Model	0.6 wt %
r (Å)	17.2
t (Å)	5.0
l (Å)	21.0
ρ_{core} (10^{-6} Å ⁻²)	-0.300
ρ_{shell} (10^{-6} Å ⁻²)	4.934
ρ_{Gly} (10^{-6} Å ⁻²)	5.806
σ_r	0.05
σ_t	0.05
σ_l	0.05
χ^2	3.90

S3. Incorporation of a structure factor to 0.6 wt % SDS in glyceline at 70 °C

The SANS profile of 0.6 wt % SDS in glyceline at $T = 70$ °C showed a possible structure factor, $S(q)$, in the low- q region of the profile. Thus, both a spherical and cylindrical form factor, $F(q)$, were trialled with a Hayter-MSA $S(q)$ (Figure S6) with fitting parameters (Table S9). Trialling an $S(q)$ in the model shows a reduction in fit quality, suggesting an $S(q)$ is not appropriate to use here. The initial increase in intensity seen in the raw SANS profile could be accounted for by the large errors indicated by the error bars.

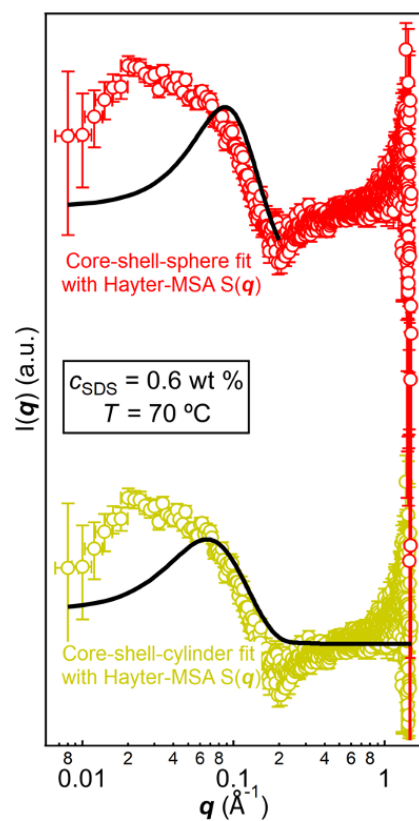


Figure S6 Fitted SANS profile for 0.6 wt % SDS in glycine at 70 °C using: a spherical model (red), and a cylindrical model (yellow) and a Hayter-MSA $S(q)$.

Table S9 Fitting parameters for the core-shell-sphere and core-shell-cylinder model with Hayter-MSA $S(q)$ used to simulate the data for 0.6 wt % *h*-SDS in *d*-glyceline at 70 °C: core radius r , shell thickness t , cylinder length l , scattering length density of the core ρ_{core} , scattering length density of the shell ρ_{shell} , scattering length density of glyceline ρ_{Gly} , volume fraction φ , charge C , temperature T , salt concentration c_{salt} , dielectric constant ϵ , polydispersity of the core radius σ_r , polydispersity of the shell thickness σ_t , polydispersity of the cylinder length σ_l , and chi squared value χ^2 .

0.6 wt % SDS	Core-Shell-Sphere Model	Core-Shell-Cylinder Model
r (Å)	16.4	17.2
t (Å)	5.0	5.0
l (Å)	--	21.0
ρ_{core} (10^{-6} Å $^{-2}$)	-0.300	-0.300
ρ_{shell} (10^{-6} Å $^{-2}$)	5.185	4.934
ρ_{Gly} (10^{-6} Å $^{-2}$)	5.742	5.806
φ	0.10	0.062
C (e)	4.99	4.36
T (K)	345	345
c_{salt} (M)	0.0	0.0
ϵ	42.7	44.7
σ_r	0.05	0.05
σ_t	0.05	0.05
σ_l	--	0.05
χ^2	29.9	5.1

S4. Model fitting analysis of SDS in glyceline at low surfactant concentrations

The scattering of the two lowest c_{SDS} measured at 70 °C was shown to be isotropic in **Figure 5a** in the main text. This was determined through fitting analysis, which yielded in a straight horizontal line (**Figure S7**). The persistence of this horizontal line through both concentrations and $T = 65$, and 70 °C, suggests these c_{SDS} contain isotropic scattering alone.

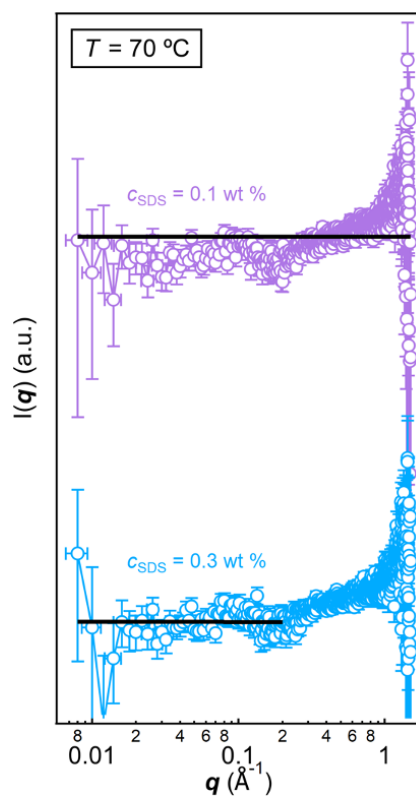


Figure S7 SANS profiles for 0.1 and 0.3 wt % *h*-SDS in *d*-glyceline at $T = 343$ K with attempted fits shown by solid black lines.

S5. Fitted SANS data for SDS in glyceline for all temperatures and concentrations

The full set of fitted data for the highest c_{SDS} is shown in the main text (**Figure 4**) with the fit parameters (**Table 1 – Table 3**). The following figures and tables will display the fits for the remaining c_{SDS} investigated for all temperatures measured.

2.7 wt % SDS in glyceline

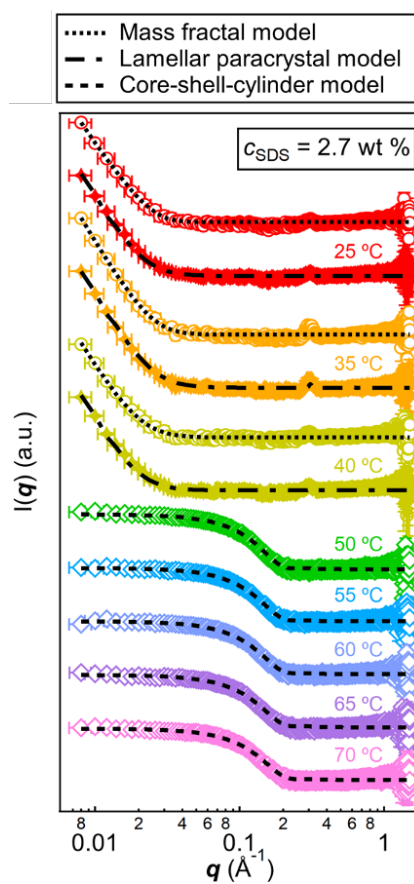


Figure S8 SANS profiles for 2.7 wt % *h*-SDS in *d*-glyceline at different temperatures. Fits to the profiles are indicated by black lines, and different lines are used to relate to the type of model used in the fit, shown in the legend; the profiles are offset on the vertical scale for clarity.

Table S10 Fitting parameters for the paracrystalline lamellar stack model used to simulate the data for 2.7 wt % *h*-SDS in *d*-glyceline at 25, 35, and 40 °C: SDS bilayer thickness t_L , number of layers in the stack n_{Layers} , d -spacing, polydispersity of the d -spacing σ_d , scattering length density of SDS ρ_{SDS} , scattering length density of glyceline ρ_{Gly} , polydispersity of the SDS bilayer thickness σ_t , and chi squared value χ^2 .

Lamellar Stack Paracrystal Model	25 °C	35 °C	40 °C
t_L (Å)	20.0	20.0	20.0
n_{Layers}	57.7	57.7	57.7
d -Spacing (Å)	20.4	20.4	20.4
σ_d (Å)	0.012	0.012	0.012
ρ_{SDS} (10^{-6} Å ⁻²)	0.427	0.436	0.354
ρ_{Gly} (10^{-6} Å ⁻²)	5.844	5.829	5.747
σ_t	1.0	1.0	1.0
χ^2	3.8	2.7	4.1

Table S11 Fitting parameters for the mass fractal model used to simulate the data for 2.7 wt % *h*-SDS in *d*-glyceline at 25, 35, and 40 °C: radius of the fractal aggregate r , fractal dimension D_m , and chi squared value χ^2 .

Mass Fractal Model	25 °C	35 °C	40 °C
r (Å)	77.5	36.1	40.0
D_m	2.91	3.00	2.98
χ^2	2.96	3.19	4.13

Table S12 Fitting parameters for the core-shell-cylinder model used to simulate the data for 2.7 wt % *h*-SDS in *d*-glyceline at 50, 55, 60, 65, and 70 °C: core radius r , shell thickness t , cylinder length l , scattering length density of the core ρ_{core} , scattering length density of the shell ρ_{shell} , scattering length density of glyceline ρ_{Gly} , polydispersity of the core radius σ_r , polydispersity of the shell thickness σ_t , polydispersity of the cylinder length σ_l , and chi squared value χ^2 .

Core-Shell-Cylinder Model	50 °C	55 °C	60 °C	65 °C	70 °C
r (Å)	18.3	18.1	18.0	17.9	16.9
t (Å)	5.0	5.0	5.0	5.0	5.0
l (Å)	25.1	24.8	24.6	24.3	23.6
ρ_{core} (10^{-6} Å ⁻²)	-0.300	-0.300	-0.300	-0.400	-0.342
ρ_{shell} (10^{-6} Å ⁻²)	4.896	4.921	4.911	4.880	4.800
ρ_{Gly} (10^{-6} Å ⁻²)	5.816	5.811	5.814	5.740	5.857
σ_r	0.05	0.05	0.05	0.05	0.05
σ_t	0.05	0.05	0.05	0.05	0.05
σ_l	0.05	0.05	0.05	0.05	0.05
χ^2	1.7	1.7	1.7	2.1	2.1

1.2 wt % SDS in glyceline

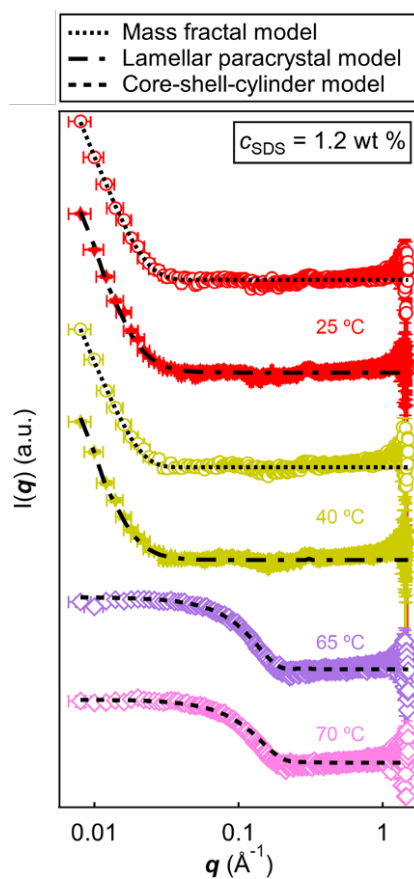


Figure S9 SANS profiles for 1.2 wt % *h*-SDS in *d*-glyceline at different temperatures. Fits to the profiles are indicated by black lines, and different lines used to relate to the type of model used in the fit, shown in the legend; the profiles are offset on the vertical scale for clarity.

Table S13 Fitting parameters for the paracrystalline lamellar stack model used to simulate the data for 1.2 wt % *h*-SDS in *d*-glyceline at 25, and 40 °C: SDS bilayer thickness t_L , number of layers in the stack n_{Layers} , *d*-spacing, polydispersity of the *d*-spacing σ_d , scattering length density of SDS ρ_{SDS} , scattering length density of glyceline ρ_{Gly} , polydispersity of the SDS bilayer thickness σ_t , and chi squared value χ^2 .

Lamellar Stack Paracrystal Model	25 °C	40 °C
t_L (Å)	20.0	20.0
n_{Layers}	57.7	57.7
<i>d</i> -Spacing (Å)	20.4	20.4
σ_d (Å)	0.012	0.012
ρ_{SDS} (10^{-6} Å^{-2})	0.425	0.326
ρ_{Gly} (10^{-6} Å^{-2})	5.852	5.811
σ_t	1.0	1.0
χ^2	4.4	7.4

Table S14 Fitting parameters for the mass fractal model used to simulate the data for 1.2 wt % *h*-SDS in *d*-glyceline at 25, and 40 °C: radius of the fractal aggregate r , fractal dimension D_m , and chi squared value χ^2 .

Mass Fractal Model	25 °C	40 °C
r (Å)	88.5	109.7
D_m	2.97	2.93
χ^2	4.4	7.5

Table S15 Fitting parameters for the core-shell-cylinder model used to simulate the data for 1.2 wt % *h*-SDS in *d*-glyceline at 65, and 70 °C: core radius r , shell thickness t , cylinder length l , scattering length density of the core ρ_{core} , scattering length density of the shell ρ_{shell} , scattering length density of glyceline ρ_{Gly} , polydispersity of the core radius σ_r , polydispersity of the shell thickness σ_t , polydispersity of the cylinder length σ_l , and chi squared value χ^2 .

Core-Shell-Cylinder Model	65 °C	70 °C
r (Å)	16.8	16.8
t (Å)	5.0	5.0
l (Å)	30.9	21.1
ρ_{core} (10^{-6} Å ⁻²)	-0.407	-0.391
ρ_{shell} (10^{-6} Å ⁻²)	4.800	4.800
ρ_{Gly} (10^{-6} Å ⁻²)	5.872	5.880
σ_r	0.05	0.05
σ_t	0.05	0.05
σ_l	0.05	0.05
χ^2	3.3	4.3

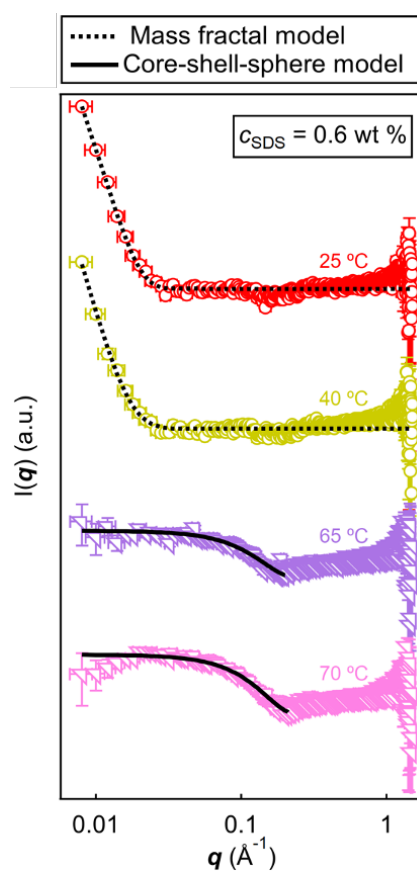


Figure S10 SANS profiles for 0.6 wt % *h*-SDS in *d*-glyceline at different temperatures. Fits to the profiles are indicated by black lines, and different lines are used to relate to the type of model used in the fit, shown in the legend; the profiles are offset on the vertical scale for clarity.

Table S16 Fitting parameters for the mass fractal model used to simulate the data for 0.6 wt % *h*-SDS in *d*-glyceline at 25, and 40 °C: radius of the fractal aggregate r , fractal dimension D_m , and chi squared value χ^2 .

Mass Fractal Model	25 °C	40 °C
r (Å)	128.5	104.5
D_m	2.65	2.89
χ^2	4.5	8.1

Table S17 Fitting parameters for the core-shell-sphere model used to simulate the data for 0.6 wt % *h*-SDS in *d*-glyceline at 65, and 70 °C: core radius r , shell thickness t , scattering length density of the core ρ_{core} , scattering length density of the shell ρ_{shell} , scattering length density of glyceline ρ_{Gly} , polydispersity of the core radius σ_r , polydispersity of the shell thickness σ_t , and chi squared value χ^2 .

Core-Shell- Sphere Model	65 °C	70 °C
r (Å)	16.5	16.4
t (Å)	4.1	5.0
ρ_{core} (10^{-6} Å ⁻²)	-0.300	-0.300
ρ_{shell} (10^{-6} Å ⁻²)	4.977	5.185
ρ_{Gly} (10^{-6} Å ⁻²)	5.784	5.742
σ_r	0.05	0.05
σ_t	0.05	0.05
χ^2	1.4	1.3

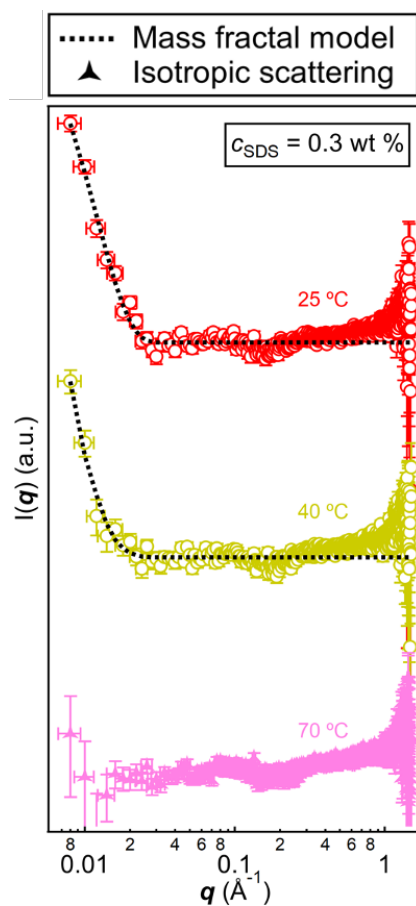


Figure S11 SANS profiles for 0.3 wt % *h*-SDS in *d*-glyceline at different temperatures. Fits to the profiles are indicated by black lines, and different lines are used to relate to the type of model used in the fit, shown in the legend; the profiles are offset on the vertical scale for clarity.

Table S18 Fitting parameters for the mass fractal model used to simulate the data for 0.3 wt % *h*-SDS in *d*-glyceline at 25, and 40 °C: radius of the fractal aggregate r , fractal dimension D_m , and chi squared value χ^2 .

Mass Fractal Model	25 °C	40 °C
r (Å)	145.6	45.8
D_m	2.30	3.22
χ^2	6.9	8.9

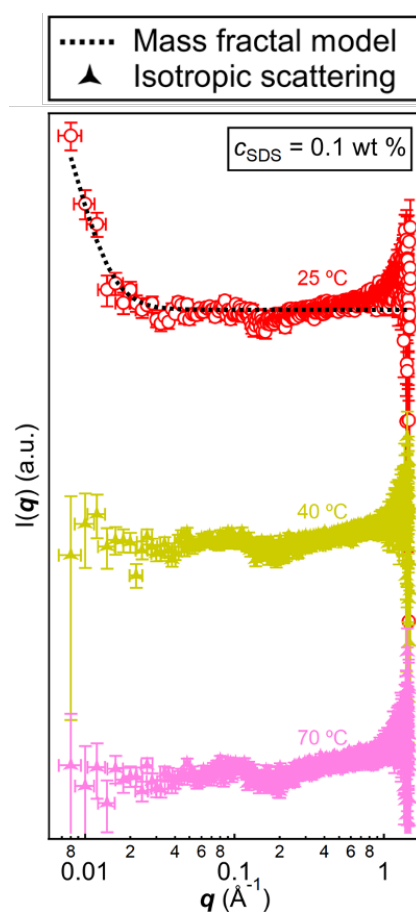


Figure S12 SANS profiles for 0.1 wt % *h*-SDS in *d*-glyceline at different temperatures. Fits to the profiles are indicated by black lines, and different lines are used to relate to the type of model used in the fit, shown in the legend; the profiles are offset on the vertical scale for clarity.

Table S19 Fitting parameters for the mass fractal model used to simulate the data for 0.3 wt % *h*-SDS in *d*-glyceline at 25 °C: radius of the fractal aggregate r , fractal dimension D_m , and chi squared value χ^2 .

Mass Fractal Model	25 °C
r (Å)	20.0
D_m	3.37
χ^2	4.9